Proc. Natl. Acad. Sci. USA
Vol. 75, No. 8, pp. 3756–3760, August 1978
Biophysics

Kinetic analysis of receptor-controlled tracer efflux from sealed membrane fragments

(acetylcholine receptor/excitable membranes/pharmacological desensitization)

JULIUS BERNHARDT AND EBERHARD NEUMANN

Max-Planck-Institut für Biochemie, D-8033 Martinsried bei München, Germany

Communicated by David Nachmansohn, June 5, 1978

ABSTRACT **A detailed kinetic analysis is presented for activator–receptor-mediated efflux of tracer substances from vesicular membrane systems in general and from sealed fragments of excitable membranes in particular. Rate constants and amplitudes, as the primary measurable quantities of the efflux kinetics, are expressed in terms of fundamental properties of vesicular membrane systems containing receptors of chemical gating systems. The experimental determination and theoretical analysis of single contributions to a complex receptor-controlled efflux has been treated for the acetylcholine receptor system; also the effect of "pharmacological densensitization" on efflux is explicitly formulated. The dependence of the measured efflux parameters on the concentration of activators can be used to derive the kinetic and thermodynamic constants for receptor activation and inactivation processes; a general kinetic scheme and two limiting cases are analyzed. The efflux of ^{22}Na from "excitable microsacs" of *Torpedo marmorata* is treated as an example, and the power of the rigorous analytical method is demonstrated. In particular, the analysis of efflux amplitudes from only a few data points offers an alternative to the longer lasting measurements for obtaining efflux curves when a safety factor is involved, as in the case of tracer ions like ^{22}Na.**

Many vital cell reactions are controlled by the interaction of cell surface receptors with small activator ligands. The study of receptors, however, entails some problems not encountered in enzyme investigations because the functional integrity of a receptor system can only be verified indirectly, by means of processes elicited by the receptor–ligand interaction (response events). Direct measurements of responses on intact cells (e.g., electrophysiological studies) are not accessible to experimental tests of molecular interactions and yield information only about the rate-limiting steps of the generation of a complex response. Intrinsic receptor properties can, in principle, be obtained by using isolated receptors. However, it is often unclear to what extent a modification of the native preparation affects the functional properties of the receptors (e.g., see ref. 1). The study of receptor-rich membrane fragments constitutes a useful intermediate stage since both kinetic investigations of activator binding as well as measurements of receptor-elicited processes are feasible. In addition, reconstitution of isolated receptors into membrane fragments is a promising technique for verifying the functional intactness of the purified protein.

Receptors are often functionally coupled to ion-translocation systems. Membrane permeability changes are thus frequently measurable responses to receptor activation. The investigation of tracer efflux from sealed membrane fragments ("microsacs") rich in acetylcholine receptors constitutes an instructive example for the study of such a receptor-mediated process.

As first shown by Kasai and Changeux (2) for *Electrophorus electricus* tissue and by Hazelbauer and Changeux (3) for *Torpedo marmorata* tissue, such membrane fragments are readily prepared from fish electric organs. A filtration assay method may be used to determine the kinetics of tracer ion efflux from microsacs loaded with tracer species (2–5). The utility of the method lies in the fact that ligand-induced receptor activation leads to an opening of transmembrane channels, which promotes tracer efflux. Receptor activator binding is thus explicitly related to efflux behavior. The measured curves represent cpm due to tracer in microsacs plotted against time, as a function of activator concentration.

Analysis of these curves is complicated by the presence of several superimposed efflux processes, of which only one is of interest (4). Furthermore, with *T. marmorata* membrane fragments, the influence of ligand-induced receptor inactivation, frequently referred to as "desensitization" (6, 7), has to be contended with. Changeux and coworkers have used a phenomenological excitability parameter, defined in terms of representative decay times, to analyze the ligand concentration dependence of their data. They obtained dose-response constants representing apparent dissociation constants for the ligand–receptor complex. Using a modified experimental procedure, Hess and coworkers (4) were able to obtain single exponential decay curves for efflux. Ligand dissociation constants were determined by fitting the rate constants for efflux to an expression involving the fraction of occupied receptors as a function of ligand concentration. For microsacs from electric eel tissue, Hess *et al.* cited no evidence that receptor inactivation influences efflux.

In the following, a general kinetic analysis of tracer efflux will be presented. It will be shown that such diverse aspects as the role of inhomogeneities in vesicle size and channel density, as well as measurable parameters connected with receptor activation and inactivation, can be cast in explicit mathematical form. In spite of the crude nature of the preparations, well-defined measurements are feasible because the physically interesting processes are mediated by units having the same functional properties (receptor systems, ion translocation channels).

METHODS

The efflux curves depicted in Fig. 1 were measured with *T. marmorata* microsacs prepared by the method of Popot *et al.* (5). The conditions under which the efflux experiments were carried out are identical to the ones cited by these authors, except for the following details. The incubation medium, as well as the dilution medium, contained 10 mM NaCl, 90 mM KCl, and 5 mM phosphate buffer (pH 7.0). These conditions ensure that competing ionic flows due to ionic gradients do not complicate the analysis of efflux events (4). The individual suctions

The costs of publication of this article were defrayed in part by the payment of page charges. This article must therefore be hereby marked "*advertisement*" in accordance with 18 U. S. C. §1734 solely to indicate this fact.

Abbreviation: BPTA, β-pyridine methyl trimethylammonium methylchloride.

were timed with six electronic clocks with switches directly coupled to the suction control levers of a Sartorius multiple suction apparatus. β-Pyridine methyl trimethylammonium methylchloride (BPTA) was synthesized according to Barlow *et al.* (8).

RESULTS

Physical Basis of Efflux Events. The measured receptor-controlled efflux process consists of a superposition of individual microsac efflux events. The specific rate of tracer ion efflux k_i, from a given microsac i, is assumed to be proportional to the number of open conductance channels:

$$k_i = \bar{\rho} S_i k' \alpha, \qquad [1]$$

where $\bar{\rho}$ is the average surface density of channels, S_i is the microsac surface area, k' is the intrinsic rate constant of efflux for one channel, and α is the fraction of open channels (4). In the absence of ionic gradients the kinetic equation describing efflux from the ith microsac is $dN_i(t)/dt = -k_i N_i(t)$, where $N_i(t)$ is the number of tracer ions in the microsac at time t. The solution is $N_i(t) = N_i(0) \exp(-k_i t)$. The quantity actually measured in efflux experiments is $P(t)$, the number of cpm due to tracer ions internal to microsacs entrapped on the filter after a suction event at time t. $P(t)$ is proportional to the sum of contributions from each microsac

$$P(t) = c \sum_i^n N_i(t) = cT_0 \sum_i^n V_i e^{-k_i t}, \qquad [2]$$

where c is a proportionality constant and n is the number of microsacs on the filter. Substituting the expression for $N_i(t)$, and noting that $N_i(0) = T_0 V_i$, where T_0 is the initial tracer concentration and V_i is the microsac volume, leads to the second equality in Eq. 2. Due to the presence of S_i in Eq. 1, k_i is implicitly volume dependent. Eq. 2 may be rewritten as

$$P(t) = cnT_0 \int V e^{-k(V)t} d\phi(V), \qquad [3]$$

where $d\phi(V) = \phi(V)\, dV$ is a differential probability; $\phi(V)$ reflects the probability of finding a microsac of volume V entrapped in the filter. For a perfectly homogeneous suspension (delta function distribution), Eq. 3 reduces to

$$\bar{P}(t) = cnT_0 \bar{V} e^{-\bar{k}t}, \qquad [4]$$

where $\bar{V}$ and $\bar{k}$ are, respectively, the average volume and rate constant.

Measurement of $P(t)$ at a given activator concentration allows the determination of two fundamental parameters:

(*i*) The rate constant of efflux, which is given as

$$\bar{k} = \bar{\rho} \bar{S} k' \alpha, \qquad [5]$$

if Eq. 4 is applicable. Deviations from this ideal relationship due to deviations of $P(t)$ from $\bar{P}(t)$ are estimated in the *Appendix*.

(*ii*) The normalized efflux amplitude E, defined by

$$E = \Delta P / P(0) = [P(0) - P(\infty)]/P(0), \qquad [6]$$

where $P(0)$ and $P(\infty)$ are the limiting values of $P(t)$ at times 0 and ∞, respectively, at a given activator concentration (see Fig. 1). If α is time independent on the time scale of the efflux process, the normalized efflux amplitude is independent of activator concentration and for $P(\infty) \ll P(0)$, $E \simeq 1$.

Information about receptor processes can be obtained from an analysis of the activator concentration dependence of the two efflux parameters $\bar{k}$ and E.

Component Contributions to Measured Efflux Curves. The curves displayed in Fig. 1 represent the efflux of ^{22}Na from *T. marmorata* microsacs. BPTA, a potent activator of acetylcholine receptors (8), was present at the concentrations indicated. These curves illustrate several characteristic features that should be dealt with in a detailed analysis. As discussed previously (2–7), the blank curve shows that considerable efflux occurs even in the absence of activator; this process is not affected by the presence of receptor inhibitors (2, 5). It follows that there is a population of microsacs that do not contain channels that can be activated, but contribute a rapid background efflux (4), characterized by an efflux rate constant k_0^f. Alternatively, some but not all of the microsacs with channels that can be activated contain permanently open efflux pores. This is plausible in view of recent evidence that preparation of membrane fragments may already entail some chemical modification of receptors (9). In contrast to the previous example, the rate constant for this contribution would then be $k^f = \bar{\rho}\bar{S}(k_0^f + \alpha k')$; see Eq. 5.

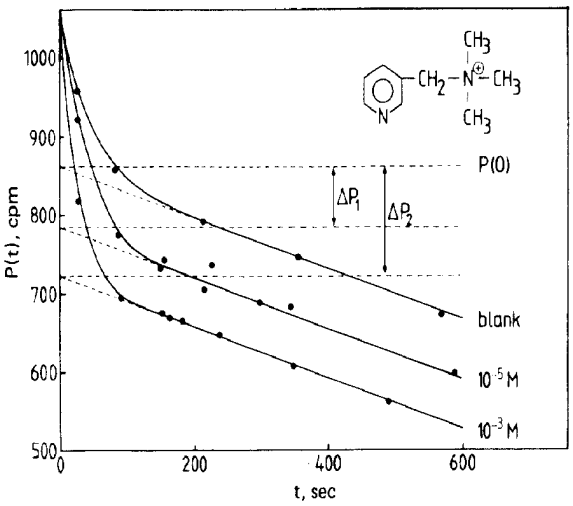

FIG. 1. Representative efflux curves for BPTA: efflux of ^{22}Na from sealed membrane fragments of *T. marmorata* in the presence of activator. The dilution bath further contained 10 mM Na^+, 90 mM K^+, and 5 mM phosphate buffer at 0°, pH 7. By means of the dashed lines a direct method is demonstrated for determining the amplitudes ΔP_1 and ΔP_2 of the receptor-controlled efflux at the indicated concentrations of activator.

After an initial rapid efflux phase the curves all attain apparently the same slope, i.e., the rapid component curve effectively has a slanted baseline. This suggests that there is a population of microsacs without channels that can be activated but that contribute a comparatively slow background efflux (4), characterized by an efflux rate constant k_0^s. All these contributions can readily be taken into account. The very slow efflux component is practically linear in the time range of interest. Back-extrapolation of this curve at receptor saturation to time zero yields the effective amplitude (in cpm) for the slow process (see Fig. 1). k_0^s can be obtained from the slope. Corrected curves can then be obtained by direct subtraction. The rapid contribution (k_0^f) could also be corrected for by adopting one of the two interpretations cited. In practice, however, one may modify the experimental procedure to deal with this contribution. As is implicit in the approach of Hess *et al.* (4), one simply has to add the required amount of activator to the dilution bath at a fixed time after the rapid efflux process has reached completion. The residual curve ($k^f = \bar{\rho}\bar{S}k'\alpha$) obtained after eliminating these superimposed contributions represents the efflux solely controlled by activator–receptor interaction.

An important finding that has not previously been noted (2–7) is the fact that the rapid efflux contribution to the curve

for 10^{-5} M BPTA (half-saturation of receptor sites) does not reach the same slanted baseline as the corresponding contribution to the curve for 10^{-3} M BPTA (saturation of receptor sites). This implies that an activator concentration-dependent *inactivation of channels* occurs because the presence of activator would otherwise necessarily lead to a complete equilibration of *all* the tracer ions in *all* microsacs that can be activated, leading to the same slanted baseline at the termination of the rapid efflux phase.

Effect of Receptor Inactivation on Efflux. Inactivation implies a time-dependent reduction of the fraction of open channels α. The kinetic equation for the activator dependent efflux contribution

$$dN(t)/dt = -\bar{k}(t) \cdot N(t) \quad [7]$$

therefore now involves a time-dependent rate coefficient

$$\bar{k}(t) = \bar{\rho}\bar{S}k' \cdot \alpha(t). \quad [8]$$

Integration of Eq. 7 leads to the solution

$$N(t) = N(0) \cdot \exp\left[-\int_0^t \bar{k}(\tau) \cdot d\tau\right], \quad [9]$$

where τ is the variable of integration.

When channel inactivation by the activator occurs on the same scale as the efflux process, the normalized efflux amplitude (see Eq. 6) is dependent on the concentration of the activator. For the time interval during which inactivation changes the initial fraction α_0 of rapidly activated receptors to the time-independent value α_∞, an amplitude exponent κ may be defined from Eqs. 6 and 9:

$$\kappa \equiv \int_0^\infty \bar{k}(\tau)d\tau = \ln\frac{N(0)}{N(\infty)} = \ln(1-E)^{-1}. \quad [10]$$

Inserting Eq. 8 into Eq. 10 yields:

$$\kappa = \bar{\rho}\bar{S}k' \int_0^\infty \alpha(\tau)d\tau. \quad [11]$$

Given a kinetic scheme relating receptor activation and inactivation to channel gating, one can use the dependence on activator concentration of the fundamental parameters $\bar{k}$ and κ, determinable from the efflux data, to obtain information about receptor processes.

Specific Models. There is considerable evidence that the acetylcholine receptor system is capable of changing among at least three different states: a closed (nonpermeable) form R, an active (open) form R′, and an inactivated (nonpermeable) state R* (10). In the time range of the efflux studies, channel activation and inactivation initiated by binding of activator A may be modelled by scheme I in Table 1. This scheme is essentially equivalent to the one presented by Katz and Thesleff (10). Electrophysiological data suggest that in the absence of activator $[R^*] \ll [R]$, and that channel activation is associated with $n > 2$ (see ref. 11).

The kinetic analysis is simplified by invoking the following assumptions: (*a*) The forms R′, R*, and A_mR, with $m < n$, are present in negligible concentrations. (*b*) The isomerizations $R \rightleftharpoons R^*$ and $A_nR' \rightleftharpoons A_nR^*$ are slow compared to the rapidly equilibrating bimolecular steps. (*c*) The fraction of open channels at the onset of inactivation, at $t = 0$, is given by $\alpha_0 = [A_nR']_0/[R_T] = [A]^n/([A]^n + K)$, where $K = [A]^n[R]/[A_nR']$ is the overall equilibrium constant for activation and $[R_T]$ is the total concentration of receptors. (*d*) Buffer conditions $[R_T] \ll [A] = [\bar{A}]$ prevail. (*e*) At the onset of inactivation, $[A_nR^*] \simeq 0$.

For scheme I in Table 1, mass conservation requires that $[A_nR^*] + [R^*] = [R_T] - ([A_nR'] + [R])$. At $t = 0$, $[R_T] = [A_nR']_0 \cdot (1 + K/[\bar{A}]^n)^{-1}$. With $K^* = [\bar{A}]^n \cdot [R^*]/[A_nR^*]$, one obtains

$$[A_nR^*] \simeq \frac{\bar{\alpha}^*}{\bar{\alpha}}([A_nR']_0 - [A_nR']), \quad [12]$$

where $\bar{\alpha} = (1 + k/[\bar{A}]^n)^{-1}$ and $\bar{\alpha}^* = (1 + K^*/[\bar{A}]^n)^{-1}$ are the equilibration factors for the rapid bimolecular equilibria.

According to Eigen (12, 13), the slow isomerization mode $d([A_nR^*] + [R^*])/dt = -d([A_nR'] + [R])/dt$ may be specified:

$$\frac{d[A_nR']}{dt} = -\bar{\alpha}\left\{\left(k_0 + k_1 \cdot \frac{K}{[\bar{A}]^n}\right)[A_nR'] - \left(k_0 + k_{-1} \cdot \frac{K^*}{[\bar{A}]^n}\right)[A_nR^*]\right\}. \quad [13]$$

Insertion of Eq. 12 and using the definitions $k_d = \bar{\alpha}(k_0 + k_1 \cdot K/[\bar{A}]^n)$, $k_{-d} = \bar{\alpha}^*(k_{-0} + k_{-1} \cdot K^*/[\bar{A}]^n)$, $\alpha = [A_nR']/[R_T]$, and $\alpha_0 = [A_nR']_0/[R_T]$, one obtains

Table 1. Kinetic schemes for receptor activation and inactivation

	Case 1	Case 2	Scheme I
	$nA + R \overset{K}{\rightleftharpoons} A_nR'$ $k_{-1} \downarrow\uparrow k_1$ A_nR^*	$nA + R \overset{K}{\rightleftharpoons} A_nR'$ $k_{-0} \downarrow\uparrow k_0$ $nA + R^* \underset{K^*}{\rightleftharpoons} A_nR^*$	$nA + R \overset{K}{\rightleftharpoons} A_nR'$ $k_{-0} \downarrow\uparrow k_0\ k_{-1} \downarrow\uparrow k_1$ $nA + R^* \underset{K^*}{\rightleftharpoons} A_nR^*$
k_d	$\bar{\alpha}k_1$	$(1-\bar{\alpha})k_0$	$\bar{\alpha}\left(k_1 + \frac{K}{[\bar{A}]^n}k_0\right)$
k_{-d}	k_{-1}	$(1-\bar{\alpha}^*)k_{-0}$	$\bar{\alpha}^*\left(k_{-1} + \frac{K^*}{[\bar{A}]^n}k_{-0}\right)$
κ	$\bar{\rho}\bar{S}\left(\frac{k'}{k_1}\right)$	$\bar{\rho}\bar{S}\left(\frac{k'}{k_0}\right)\frac{[\bar{A}]^n}{K}$	$\bar{\rho}\bar{S}\left(\frac{k'}{k_1}\right)\frac{[\bar{A}]^n}{[\bar{A}]^n + K\left(\frac{k_0}{k_1}\right)}$

The expressions in each row reflect the apparent rate coefficients k_d and k_{-d} of inactivation and the amplitude exponent κ; note that $\bar{\alpha} \simeq \alpha_0$ (buffer condition for the activator).

$$\frac{d\alpha(t)}{dt} = -\frac{1}{\tau_d}\alpha(t) + k_{-d}\cdot\alpha_0, \qquad [14]$$

where $\tau_d = (k_d + k_{-d})^{-1}$ is the relaxation time for the inactivation process. The specific expressions for k_d and k_{-d} for scheme I and the limit cases 1 and 2, respectively, are summarized in Table 1.

Integration of Eq. 14 results in an expression for the fraction of open channels, subsequent to rapid activation,

$$\alpha(t) = \alpha_0\{B + (1 - B)\exp(-t/\tau_d)\}, \qquad [15]$$

where $B = (1 + k_d/k_{-d})^{-1}$. When the inactivation reaction is equilibrated, $d\alpha(t)/dt = 0$ and $\alpha(t \to \infty) = \alpha_\infty = \alpha_0 \cdot B$, being dependent on the activator concentration.

For the specific example of the acetylcholine receptor system, $k_d \gg k_{-d}$ (10), so that Eq. 15 may be approximated as $\alpha(t) \simeq \alpha_0 \cdot \exp(-k_d \cdot t)$. Substitution into Eqs. 8 and 11 yields:

$$\bar{k} \simeq \bar{\rho}\bar{S}k' \cdot \alpha_0 \cdot \exp(-k_d \cdot t) \qquad [16]$$

$$\kappa \simeq \bar{\rho}\bar{S}k' \cdot \alpha_0 \cdot k_d^{-1}. \qquad [17]$$

It is noteworthy that case 1, case 2, and scheme I in Table 1 can be distinguished on the basis of the dependence of the amplitude exponent κ on the activator concentration, alone (see Fig. 2).

DISCUSSION

Two relevant parameters related to efflux can be determined from the receptor-controlled efflux contribution: the normalized efflux amplitude E and the rate coefficient $\bar{k}$. E is directly determinable from a plot of $P(t)$ against time (see Fig. 1); $\bar{k}$ is given as the slope of a plot of $\ln P(t)$ against time. In the absence of inactivation, the time dependence of $P(t)$ is given by the ideal exponential relationship of Eq. 4. Inhomogeneities in microsac size will generally lead to deviations from strict exponential behavior (see *Appendix*). When inactivation occurs, $\bar{k}$ is itself time dependent.

Information about receptor processes can be determined from the activator concentration dependence of the fraction of open channels α. It is then necessary to assume a kinetic scheme for receptor involvement in channel gating. In the absence of inactivation, the dependence of $\bar{k}$ on $[\bar{A}]$, Eq. 5, with $\alpha = (1 + K/[\bar{A}]^n)^{-1}$ may be used to establish the value of n and the overall dissociation constant K for activator binding to the active receptor state (e.g., see ref. 4). If inactivation occurs, the analysis is more complicated. The value of $\bar{k}$ extrapolated to zero time (addition of activator) given by $\bar{k}(0) = \bar{\rho}\bar{S}k'$ $\alpha(0)$ may then be used to determine intrinsic parameters of the receptor system. The dependence of both $\bar{k}$ and κ on activator concentration can be used to evaluate not only the binding constant to the active form, but also kinetic and thermodynamic parameters for inactivation.

Qualitative inspection of the dependence of κ on $[\bar{A}]$ alone suffices to exclude certain specific reaction mechanisms (see Table 1). For case 1, κ is concentration independent; case 2 predicts a linear dependence of κ on $[\bar{A}]^n$, and the general scheme shows saturation after a linear range for small $[\bar{A}]^n$. Thus, a general analysis of efflux data complemented by specific models for receptor-mediated permeability changes can be used to study receptor functions on the level of sealed membrane fragments.

For *Torpedo* and eel microsacs, efflux studies are practically feasible because the pre-exponential factors in Eq. 4 lead to a measurable amplitude and because the factors $\bar{\rho}$, $\bar{S}$, and k' in Eq. 5 multiply to yield a measurable $\bar{k}$. The original experimental approach of Changeux and colleagues (2, 5) leads to composite efflux curves, in which a rapid efflux process, not controlled by receptors, is superimposed on the receptor-controlled component. The analysis of component efflux contributions presented above has shown that the determination of well-defined kinetic and thermodynamic receptor properties requires a resolution of the receptor-controlled component curve. This raises a practical difficulty in that the corresponding curve is generally steeper than the composite curve (e.g., see ref. 4). More measurements are thus required to obtain accurate results. However, this makes the method unsuitable for routine investigations due to the safety factor involved in working with the candidate tracer ions (e.g., ^{22}Na).

The aim of citing data for the specific activator BPTA was mainly to illustrate key factors that must be accounted for in a detailed analysis. As demonstrated in Fig. 2, the induced-fit model (case 1) and also case 2 in Table 1 are not adequate to describe the inactivation of the acetylcholine receptor promoted by BPTA binding. The full scheme I is necessary to model BPTA-induced inactivation. At present, it is, however, not possible to give reliable values for the rate coefficients because the resolution of the respective efflux component is not sufficient. Finally, the derivation presented above is sufficiently

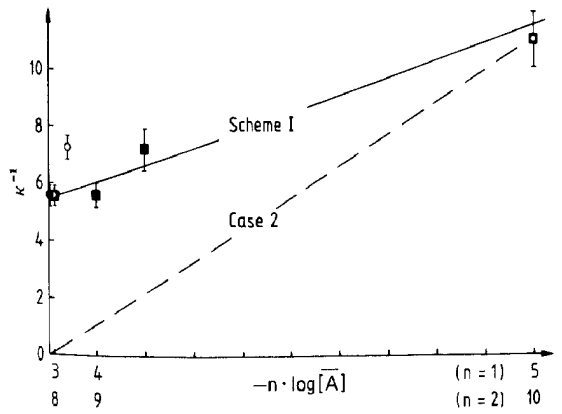

FIG. 2. Evaluation of efflux data (partially represented in Fig. 1) according to Eq. 17 and Table 1. Case 1 can be excluded beforehand. Case 2 predicts that $1/\kappa = 0$ at $[\bar{A}] \to \infty$, and can be eliminated too. Only scheme I, where $\kappa^{-1} = k_1(\bar{\rho}\bar{S}k')^{-1} \cdot (1 + Kk_0k^{-1}[\bar{A}]^{-n})$ has a finite intercept, is adequate for BPTA-induced inactivation. ■, n = 1; ○, n = 2.

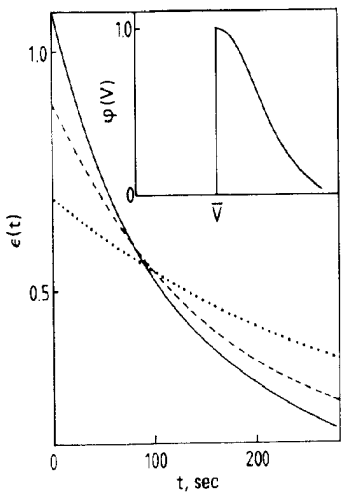

FIG. 3. The error term $\epsilon(t)$, defined by Eq. A2, as a function of time. The three curves refer to different standard deviations σ_v from mean volume $\bar{V}$: (——) $\sigma_v = 1.5\ \bar{V}$; (- - - - - - -) $\sigma_v = \bar{V}$; (. . . . . .) $\sigma_v = 0.5\ \bar{V}$. The representative values $\bar{V} = (0.001)\ (4\pi/3)\ \mu m^3$ and $\bar{k} = 0.01\ sec^{-1}$ were used in each case. (*Inset*) General form of the volume distribution $\phi(V)$ used to model $d\phi(V) = \phi(V)dV$ in Eq. A1.

general to be applicable to any efflux process controlled by a gating macromolecule.

APPENDIX

If there is an inhomogeneity in the size of the microsacs, deviations from the ideal relationship (Eq. 4) for $\bar{P}(t)$ are expected. It is of interest to determine the magnitude of the error involved. From the general expression Eq. 3, one has $P(t) = \epsilon(t)\bar{P}(t)$. The correction factor $\epsilon(t) = P(t)/\bar{P}(t)$ is given by

$$\epsilon(t) = \int (V/\bar{V}) \exp\{[\bar{k} - k(V)]t\} d\phi(V). \quad [A1]$$

One may estimate this quantity by assuming that the microsacs are spherical so that the surface area term in Eq. 5 is given by $S = 3(4\pi/3)^{1/3}V^{2/3}$, and the distribution $\phi(V)$ in $d\phi(V) = \phi(V)/dV$ may be modelled as half of a Gaussian distribution (*inset*, Fig. 3), to account for the cutoff of the filter. $\epsilon(t)$ is then given by

$$\epsilon(t) = \frac{1}{\sqrt{2\pi\sigma_v^2}} \int_0^\infty \frac{V + \bar{V}}{\bar{V}} \times \exp\left\{\left[1 - \left(\frac{V + \bar{V}}{\bar{V}}\right)^{2/3}\right]\bar{k}t - \frac{V^2}{2\sigma_v^2}\right\} dV. \quad [A2]$$

The quantity σ_v represents the standard deviation of the volume from $\bar{V}$.

Numerical integration of Eq. A2 for representative values of $\bar{V}$, $\bar{k}$, and σ_v leads to the curves depicted in Fig. 3. For $\sigma_v = 1.5\bar{V}$, a least squares fit leads to the relationship

$$\ln \epsilon(t) \approx 9.349 \times 10^{-2} - 8.106 \times 10^{-3}t + 8.077 \times 10^{-6}t^2. \quad [A3]$$

Clearly, the time dependence of the correction term is not purely exponential. Thus, errors due to size heterogeneity cannot easily be corrected for.

We thank Prof. Nachmansohn for critical comments and U. Wolfänger for her able assistance.

1. Neumann, E. & Bernhardt, J. (1977) *Annu. Rev. Biochem.* **46**, 117–141.
2. Kasai, M. & Changeux, J.-P. (1971) *J. Membr. Biol.* **6**, 1–23.
3. Hazelbauer, G. L. & Changeux, J.-P. (1974) *Proc. Natl. Acad. Sci. USA* **71**, 1479–1483.
4. Hess, G., Andrews, J. P., Struve, G. E. & Coombs, S. E. (1975) *Proc. Natl. Acad. Sci. USA* **72**, 4371–4375.
5. Popot, J.-L., Sugiyama, H. & Changeux, J.-P. (1976) *J. Mol. Biol.* **106**, 469–483.
6. Sugiyama, H., Popot, J.-L. & Changeux, J.-P. (1976) *J. Mol. Biol.* **106**, 485–496.
7. Popot, J.-L., Sugiyama, H. & Changeux, J.-P. (1974) *C. R. Hebd. Seances Acad. Sci. Ser. D* **279**, 1721–1724.
8. Barlow, R. B., Thompson, G. M. & Scott, N. C. (1969) *Br. J. Pharmacol.* **37**, 555–584.
9. Chang, H. W. & Bock, E. (1977) *Biochemistry* **16**, 4513–4520.
10. Katz, B. & Thesleff, S. (1957) *J. Physiol.* **138**, 63–80.
11. Sheridan, R. E. & Lester, H. A. (1975) *Proc. Natl. Acad. Sci. USA* **72**, 3496–3500.
12. Eigen, M. (1967) *Nobel Symp.* **5**, 333–367.
13. Eigen, M. (1968) *Q. Rev. Biophys.* **1**, 3–33.